Scientia Iranica B (2015) 22(2), 493–503

Sharif University of Technology
Scientia Iranica
Transactions B: Mechanical Engineering
www.scientiairanica.com

Mechanical analysis of a functionally graded cylinder-piston under internal pressure due to a combustion engine using a cylindrical super element and considering thermal loading

R. Pourhamid[a], M.T. Ahmadian[b,*], H. Mahdavy Moghaddam[a] and A.R. Mohammadzadeh[a]

a. *Department of Mechanical and Aerospace Engineering, Science and Research Branch, Islamic Azad University, Tehran, Iran.*
b. *School of Mechanical Engineering, Sharif University of Technology, Tehran, Iran.*

Received 27 April 2014; received in revised form 22 July 2014; accepted 17 November 2014

KEYWORDS
Super Element Method (SEM);
Mechanical analysis and thermal loading;
Functionally graded material;
Cylinder;
Piston.

Abstract. Increasing the performance of combustion engines has always been of interest to engine designers. In this regard, one approach has been to implement newly developed materials. Functionally Graded Materials (FGMs) have been shown to be heat treatable materials for high-temperature environments with thermal protection. Using these materials requires an understanding of the development of temperature and stress distribution in the transient state. This information is considered to be the main key in the design and optimization of devices for failure prevention. In this paper, a cylindrical Super Element (SE) has been employed to investigate the mechanical stress distribution of a cylinder-piston mechanism made of FGM for a combustion engine design. Analysis indicates that modeling a cylinder and piston with a few super elements gives the same results as a conventional finite element with 10052 elements. Materials are selected to be ceramics and metal with power low distribution. Results indicate that temperature distribution in the thickness of the cylinder does not vary, as the power of material distribution exceeds the value of one, while temperature distribution variation is sensitive to power distribution less than one. This has a high effect on stress distribution in both FG cylinders and FG pistons.

1. Introduction

Functionally Graded Materials (FGMs) are modern inhomogeneous materials in which two or more different material ingredients change continuously and gradually resulting in elimination of interface problems and, consequently, uniformity of stress and temperature distribution. Frequently, these materials are made from ceramic and metal. Usually, the composition varies from a ceramic-rich surface to a metal-rich surface. This behavior is according to a desired variation of the volume fraction. These changes are considered as power or exponential functions in the radius or thickness directions [1-3].

This material can be used in various industrial applications, such as engine components, especially in cylinder blocks and pistons. The application of FGMs can be an inventive phenomenon in internal combustion engines [4], but, until now, FGM has not been used in the industry of internal combustion engines. However,

*. *Corresponding author. Tel.: +98 21 66165503;*
Fax: +98 21 66000021
E-mail address: ahmadian@sharif.edu (M.T. Ahmadian)

if we consider the thermal barrier coating system as a type of FGM, they were used in Cummins engines, commercially [5].

The FGM structure with ceramic is usually preferred in the design of pistons and cylinders because of the preference in thermal barrier and wear resistance. In recent years, scientists have presented several pieces of research on thermal and stress analyses of FGMs, using semi-analytical and numerical methods. Arefi [6] presented the nonlinear thermo-elastic analysis of a thick-walled functionally graded piezoelectric cylinder under thermal, mechanical and electrical loads. He proposed a novel analytical method for estimating the response of systems of nonlinear differential equations based on the modification and combination of Adomian's decomposition and successive approximation methods.

Dai and Rao [7] studied the dynamic thermoelastic behavior of a double-layered hollow cylinder with an FGM layer. They utilized the finite difference method and the Newmark method to solve the problem under both dynamic mechanical and thermal loads. Feng et al. [8] presented the thermo-mechanical analysis of FG cylindrical vessels, using an edge-based smoothed Finite Element Method (FEM). In this method, the problem domain was firstly discretized into triangular elements, and edge-based smoothing domains were further formed along the edges of triangular meshes. In order to improve the accuracy, stiffness matrices were calculated using a strain smoothing technique in the smoothing domains. Nie and Batra [9-10] presented material analysis of FG isotropic and incompressible linear elastic hollow cylinders. They used the Airy stress function to derive exact solutions for plane strain deformations.

Safari et al. [11] conducted two-dimensional dynamic analysis of thermal stresses in a finite-length FG thick hollow cylinder, subjected to thermal shock loading. Using the Laplace transform and the series solution, thermo-elastic Navier equations in the displacement form were solved analytically. Desai and Kant [12] presented a mixed semi-analytical solution for FG finite length cylinders of orthotropic materials, subjected to thermal loads. In this research, boundary conditions were satisfied exactly by taking an analytical expression in terms of the Fourier series expansion. First order simultaneous ordinary differential equations were obtained as the mathematical model, which were integrated through an effective numerical integration technique by first transforming the boundary value problem into a set of initial value problems. Asemi et al. [13] carried out the dynamic analysis of thick short length FG cylinders. In this article, the Finite Element Method (FEM), based on the Rayleigh-Ritz energy formulation, was applied. Besides, the Newmark direct integration method was also used to solve time dependent equations. Darabseh et al. [14] presented the transient thermo-elasticity analysis of a FG thick hollow cylinder, based on the Green-Lindsay model. The heat conduction equation and the equation of motion were solved using the Galerkin finite element method. Investigating the thermal analysis of FG cylinders and FG pistons in the application of FGMs in internal combustion engines is very rare. Akhlaghi et al. [15] studied heat loss and thermal stress in direct injection diesel engines, using FGMs. They used a combination of finite element and finite difference methods.

Due to the high computational time of the conventional finite element method, researchers have tried to develop super elements to overcome this problem. Koko and Olson [16] developed a super element to analyze stress distribution in a plate. Ahmadian and Zangane [17] used a super element to perform the free vibration analysis of laminated stiffened plates. Ahmadian and Bonakdar [18] developed a cylindrical super element to performed structural analysis of a laminated hollow cylinder. Taghvaeipour et al. [19] presented the new cylindrical element formulation for the vibration analysis of FGM hollow cylinders. They have shown that the super element is a capable cylinder, is accurate enough, and is much less time consuming.

In this paper, stress analysis of a FGM cylinder and piston under combustion pressure, considering thermal stresses, is performed. SEM is implemented to analyze the mechanical behavior of both FG cylinders and pistons in a transient state. Materials are assumed to vary in the radial direction of the cylinder and the longitudinal direction of the piston. To validate the results, a simple case of uniform material distribution, metal and ceramic results of the super element, is compared with ABAQUS software modeling and very good results were obtained. The distribution of the material is based on the power low method, and by applying the super element, mechanical analysis of the FGM cylinder is evaluated.

2. Formulation and modeling

Governing equations for the cylinder and piston are developed using an energy approach, and, consequently, an appropriated code is developed using MATLAB software.

The shape function for the SE before implementing this element into the equation of motion should be defined. A super element is shown in Figure 1 with 16 nodes. In this figure, r, α and z are radial, tangential and axial coordinates, respectively.

Considering global and local coordinate systems, the relation between these coordinates may be expressed as follows:

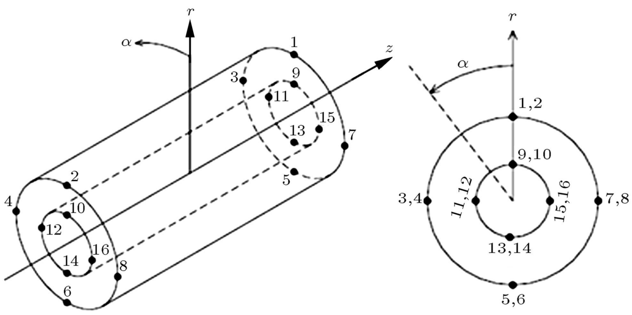

Figure 1. The super element with 16 nodes.

$$\eta = \frac{2r - (r_i + r_o)}{r_o - r_i}, \tag{1}$$

$$\lambda = \frac{\alpha}{\pi} - 1, \tag{2}$$

$$\xi = \frac{2z}{l}, \tag{3}$$

$$N_i(\xi, \eta, \lambda) = \tilde{f}_i(\eta, \lambda, \xi), \tag{4}$$

where L is the super element length, and r_i and r_o are inner and outer radii of the geometry.

The specific shape functions for this element are given in the Appendix.

2.1. Stress analysis

The relation between the strain and the displacement could be written as follows [18]:

$$\{\varepsilon\}_{6\times1} = [d]_{6\times3}\{u\}_{3\times1}, \tag{5}$$

where:

$$\{\varepsilon\} = \left\{\varepsilon_{rr} \quad \varepsilon_{\alpha\alpha} \quad \varepsilon_{zz} \quad \gamma_{r\alpha} \quad \gamma_{rz} \quad \gamma_{\alpha z}\right\}^T, \tag{6}$$

$$\{u\} = \left\{u_r \quad u_\alpha \quad u_z\right\}^T. \tag{7}$$

And, since the strains can be related to the components of the displacement vector as [18]:

$$\varepsilon_{rr} = \frac{\partial u_r}{\partial r}, \qquad \varepsilon_{\alpha\alpha} = \frac{u_r}{r} + \frac{1}{r}\frac{\partial u_\alpha}{\partial \alpha},$$

$$\varepsilon_{zz} = \frac{\partial u_z}{\partial z}, \tag{8}$$

$$\gamma_{r\alpha} = \frac{1}{r}\frac{\partial u_r}{\partial \alpha} + \frac{\partial u_\alpha}{\partial r} - \frac{u_\alpha}{r},$$

$$\gamma_{rz} = \frac{\partial u_r}{\partial z} + \frac{\partial u_z}{r},$$

$$\gamma_{\alpha z} = \frac{\partial u_\alpha}{\partial z} + \frac{1}{r}\frac{\partial u_z}{\partial \alpha}. \tag{9}$$

The d matrix is achieved as:

$$[d] = \begin{bmatrix} \frac{\partial}{\partial r} & 0 & 0 \\ \frac{1}{r} & \frac{1}{r}\frac{\partial}{\partial \alpha} & 0 \\ 0 & 0 & \frac{\partial}{\partial z} \\ \frac{1}{r}\frac{\partial}{\partial \alpha} & \frac{\partial}{\partial r} - \frac{1}{r} & 0 \\ \frac{\partial}{\partial z} & 0 & \frac{\partial}{\partial r} \\ 0 & \frac{\partial}{\partial z} & \frac{1}{r}\frac{\partial}{\partial \alpha} \end{bmatrix}. \tag{10}$$

The strain energy associated with this system can be written as [20]:

$$\Pi = \int_v \{\varepsilon\}^T\{\sigma\}dv - \int_s \{u\}^T \{\tilde{p}\}\, ds, \tag{11}$$

where:

$$\{\tilde{p}\} = \left\{\tilde{p}_r \quad \tilde{p}_\alpha \quad \tilde{p}_z\right\}^T, \tag{12}$$

$$\{\sigma\} = \left\{\sigma_{rr}\sigma_{\alpha\alpha}\sigma_{zz}\tau_{r\alpha}\tau_{rz}\tau_{\alpha z}\right\}^T, \tag{13}$$

where $\{\tilde{p}\}$ is the combustion pressure and $\{\sigma\}$ is the stress note.

Due to the principle of minimum total potential energy, the differential state of this energy should be zero ($\delta\Pi = 0$). Hence, considering Eq. (5) and the Kantorovich approximation for the displacement ($\{u\}_{3\times1} = [\tilde{N}]_{3\times48}\{u^{(e)}\}_{48\times1}$), Eq. (11) could be reduced to the following equation:

$$\int_v [B]^T\{\sigma\}dv - \int_s \left[\tilde{N}\right]^T \{\tilde{p}\}\, ds = 0, \tag{14}$$

where:

$$[B]_{6\times48} = [d]_{6\times3}\left[\tilde{N}\right]_{3\times48}, \tag{15}$$

$$\left[\tilde{N}\right] = \begin{bmatrix} N1 & 0 & 0 & \cdots & N16 & 0 & 0 \\ 0 & N1 & 0 & \cdots & 0 & N16 & 0 \\ 0 & 0 & N1 & \cdots & 0 & 0 & N16 \end{bmatrix}, \tag{16}$$

$$[B] = \begin{bmatrix} N_{1,r} & 0 & 0 & \cdots & N_{16,r} & 0 & 0 \\ \frac{N_1}{r} & \frac{N_{1,\alpha}}{r} & 0 & \cdots & \frac{N_{16}}{r} & \frac{N_{16,\alpha}}{r} & 0 \\ 0 & 0 & N_{1,z} & \cdots & 0 & 0 & N_{16,z} \\ \frac{N_{1,\alpha}}{r} & N_{1,r} - \frac{N_1}{r} & 0 & \cdots & \frac{N_{16,\alpha}}{r} & N_{16,r} - \frac{N_{16}}{r} & 0 \\ N_{1,z} & 0 & N_{1,r} & \cdots & N_{16,z} & 0 & N_{16,r} \\ 0 & N_{1,z} & \frac{N_{1,\alpha}}{r} & \cdots & 0 & N_{16,z} & \frac{N_{16,\alpha}}{r} \end{bmatrix}. \tag{17}$$

According to Hook's law, the relation between stress and strain could be considered as [18]:

$$\{\sigma\}_{6\times 1} = [D]_{6\times 6}(\{\varepsilon\} - \{\varepsilon_T\})_{6\times 1}, \tag{18}$$

where:

$$\{\varepsilon_T\} = \left\{\alpha_T\Delta T \quad \alpha_T\Delta T \quad \alpha_T\Delta T \quad 0 \quad 0 \quad 0\right\}^T, \tag{19}$$

$$[D] = \frac{E}{(1+\nu)(1-2\nu)}$$

$$\begin{bmatrix} 1-\nu & \nu & \nu & 0 & 0 & 0 \\ \nu & 1-\nu & \nu & 0 & 0 & 0 \\ \nu & \nu & 1-\nu & 0 & 0 & 0 \\ 0 & 0 & 0 & \frac{1-2\nu}{2} & 0 & 0 \\ 0 & 0 & 0 & 0 & \frac{1-2\nu}{2} & 0 \\ 0 & 0 & 0 & 0 & 0 & \frac{1-2\nu}{2} \end{bmatrix}, \tag{20}$$

in which α_T, ΔT, E and v are the thermal expansion coefficient, temperature difference, elastic modulus and Poisson ratio, respectively.

Thus, Eq. (14) could be represented as follows:

$$\int_v [B]^T[D]\left([B]\left\{u^{(e)}\right\} - \{\varepsilon_T\}\right)dv - \int_s [N]^T\{\tilde{p}\}\,ds = 0. \tag{21}$$

Then, the governing equation could be simplified as follows:

$$\left[\tilde{k}^{(e)}\right]\left\{u^{(e)}\right\} = \left\{\tilde{f}^{(e)}\right\}, \tag{22}$$

$$\left[\tilde{k}^{(e)}\right] = \int_v [B]^T[D][B]dv, \tag{23}$$

$$\left[\tilde{f}^{(e)}\right] = \int_v [B]^T[D]\{\varepsilon_T\}dv + \int_s \left[\tilde{N}\right]^T\{\tilde{p}\}\,ds. \tag{24}$$

Boundary conditions for the cylinder could be mentioned as follows:

$$\begin{aligned} u_z &= o \quad && \text{at} \quad z = \pm L/2, \\ u_r &= o \quad && \text{at} \quad z = \pm L/2, \quad r = r_o, \\ \sigma_{rr} &= -p \quad && \text{at} \quad r = r_i, \\ \sigma_{rr} &= 0 \quad && \text{at} \quad r = r_o, \end{aligned} \tag{25}$$

where p is the combustion pressure. Here, it is assumed that the top and bottom areas of the cylinder are in a fixed condition (in the direction of z) in connection with the cylinder head and the oil pan in the engine. To prevent the cylinder motion in the direction of the combustion pressure, the motion of the outer radius in the top and bottom of the cylinder is assumed to be zero. In addition, it is assumed that there is no contraction between the cylinder and piston.

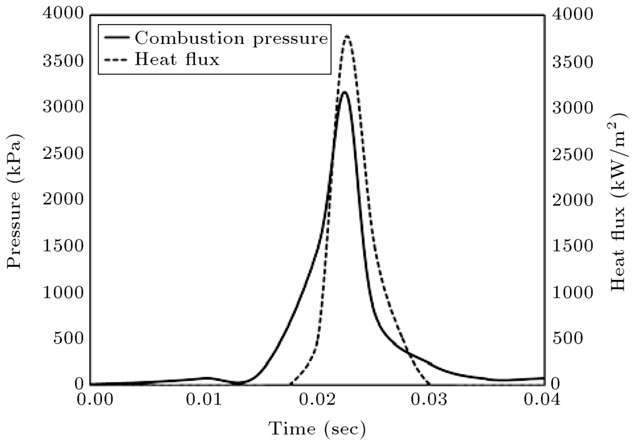

Figure 2. The combustion pressure and the heat flux versus the time.

Boundary conditions for the piston are assumed to be:

$$\begin{aligned} u_z &= o \quad && \text{at} \quad z = -L/2, \\ \sigma_{zz} &= -p \quad && \text{at} \quad z = +L/2, \\ \sigma_{rr} &= 0 \quad && \text{at} \quad z = -L/2. \end{aligned} \tag{26}$$

The force from the connecting rod to the piston is neglected here. Instead, it is assumed that the bottom area of the piston is in a fixed condition (in the direction of z).

2.2. Load conditions

The combustion pressure and heat generation due to combustion in the cylinder are shown in Figure 2. In this figure, the combustion pressure and heat generation versus time, for a complete crank shaft cycle (720 degrees), at an engine speed of 3000 rpm, is plotted. The maximum pressure is considered to be 3161.3 kPa, which occurred after about 0.02 sec of the combustion process.

Temperature distribution within the cylinder, and thickness is given by Figure 3(a), while the temperature distribution in the piston length is presented by Figure 3(b). The temperature distribution is evaluated based on the heat flux of the engine [22].

2.3. Geometry and properties

The geometric dimensions of the cylinder and piston for the engine are as follows:

- Piston radius: 71 mm;
- Piston length: 27.9 mm;
- Cylinder inner radius: 71 mm;
- Cylinder outer radius: 81 mm;
- Cylinder length: 83.6 mm.

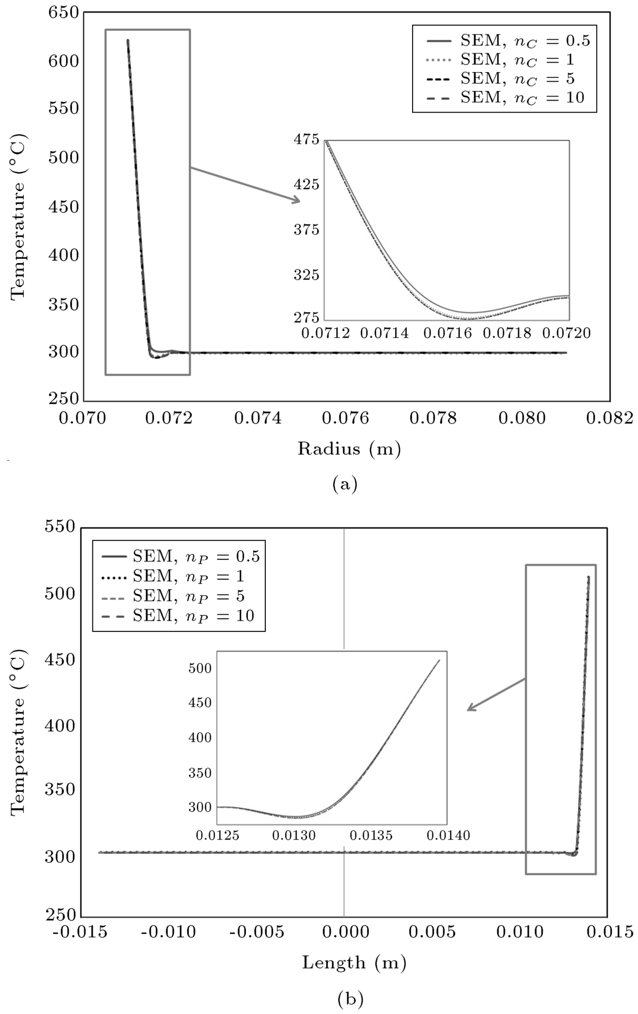

Figure 3. Temperature distribution for (a) FG cylinder, and (b) FG piston.

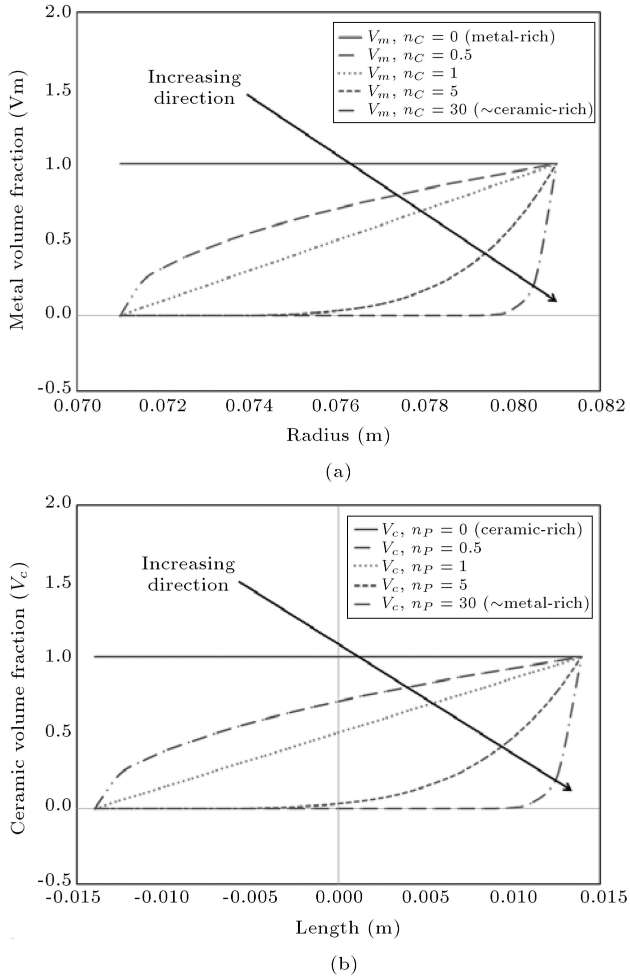

Figure 4. Distribution of the (a) metal volume fraction versus the radius of the cylinder, and (b) ceramic volume fraction versus the length of the piston.

The material structure for the cylinder is assumed to start as ceramic at the inner surface and gradually changes to metal at the outer surface. For the piston, it starts as ceramic at the top surface in contact with combustion and changes gradually to metal at the bottom surface.

The material profile for the cylinder and piston is assumed to have a power low distribution starting from ceramic and ending with metal; inside-out for the cylinder (Eq. (27)) and top to bottom for the piston (Eq. (28)):

$$v_m(r) = \left(\frac{r - r_i}{r_o - r_i}\right)^{n_c}, \qquad v_c(r) = 1 - v_m(r), \quad (27)$$

$$v_c(z) = \left(\frac{2z - L}{2L}\right)^{n_p}, \qquad v_m(z) = 1 - v_c(z), \quad (28)$$

where V_m and V_c are metal and ceramic volume fractions, respectively. The mechanical and physical properties of the material (P) for the cylinder and piston may be written as follows:

$$p(T, r) = p_m(T)v_m(r) + p_c(T)v_c(r), \quad (29)$$

$$p(T, z) = p_m(T)v_m(z) + p_c(T)v_c(z), \quad (30)$$

in which P_m and P_c are metal and ceramic properties, respectively. Figure 4(a) and (b) represent metal volume fraction versus the radius of the cylinder and ceramic volume fraction versus the length of the piston, respectively.

The mechanical and physical properties of the metal (Ti-6Al-4V) and ceramic (Si_3N_4) are presented in Table 1. It should be mentioned that titanium alloy (Ti-6Al-4V) is of great interest to car manufacturers in engine design.

2.4. Validation process

To validate the results obtained by the super element, conventional finite element software is used for simple cases of a metal-rich state and for a ceramic-rich condition. For the axisymmetric cylinder and

Table 1. Material properties for the studied FGM.

Characteristics	Metal (Ti-6Al-4V)	Ceramic (Si_3N_4)
ρ $\left(\frac{\text{kg}}{\text{m}^2}\right)$	2370	4429
c_p $\left(\frac{\text{J}}{\text{kg}^\circ\text{K}}\right)$	625.30	555.11
k $\left(\frac{\text{W}}{\text{m}^\circ\text{K}}\right)$	13.72	1.21
E (GPa)	122.56	348.43
v (-)	0.29	0.24
α_T $\left(\frac{1}{^\circ\text{K}}\right)$	7.58×10^{-6}	5.87×10^{-6}

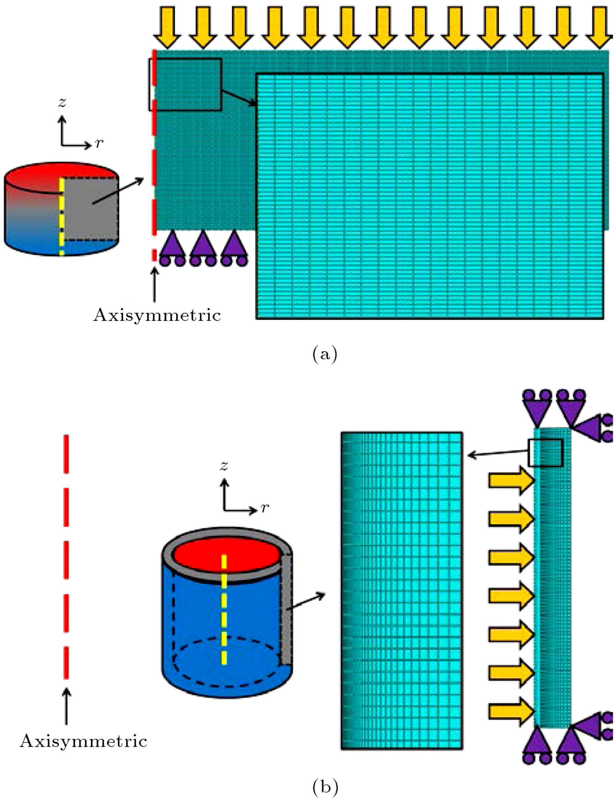

Figure 5. FE models of (a) the piston and (b) the cylinder in the ABAQUS software.

piston, the minimum number of elements and nodes for the convergence are chosen to be 2100 finite elements, with 2210 nodes for the cylinder and 7952 finite elements, with 8136 nodes for the piston (Figure 5).

3. Results and discussion

3.1. Convergency for cylinder

Convergence of the results for a metal-rich ($n = 0$) cylinder using a super element is presented in Figure 6. As the number of super elements increases beyond 20, the stress distribution variation is minimal.

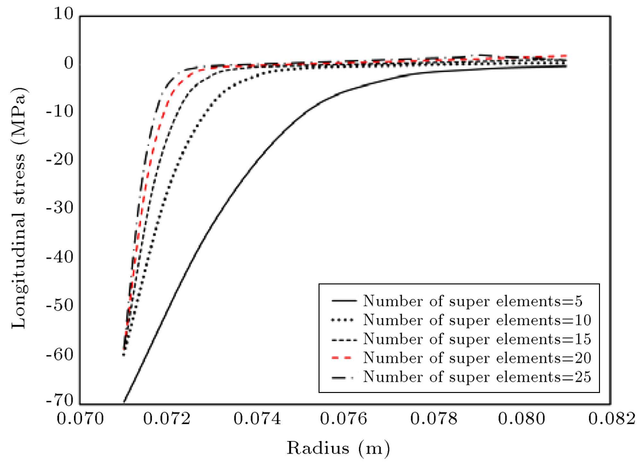

Figure 6. Distribution of the longitudinal stress in the metal-rich cylinder for different numbers of super elements.

3.2. Validation for cylinder

Stress distribution from the inside-out, in an axial direction, for metal-rich and ceramic-rich, based on a super element with 20 elements and conventional finite element analysis at the top of the cylinder, are presented in Figure 7. Results for the two methods are the same with maximum difference of 2% while the computational time with super element is much less than the conventional finite element. Stress distribution in radial and longitudinal are presented in Figure 8(a) and (b), respectively.

Distribution of radial stress (in the mid-length of the cylinder) is uniform and changes gradually through the radius. The longitudinal stress is compressive inside the cylinder and changes to tensile in the radial direction. In addition, the value of the radial stress is lower than the value of the longitudinal stress, far from the boundary. The stress value in ceramic-rich materials is higher than that of metal-rich materials. This is due to the higher value of modulus elasticity (Table 1).

3.3. Convergency for piston

The radial stress distribution of the metal-rich piston ($n = 0$) is depicted in Figure 9. As the number of super elements along the length of the piston used in the model increases, the radial stress gradient increases. Based on the convergency test, it is found that 40 super elements (with 328 nodes) in the length direction of the piston have enough accuracy for correct radial stress distribution.

3.4. Validation for piston

Stress distribution from the top to bottom and in a radial direction with metal-rich and ceramic-rich materials, based on a super element with 40 elements and with conventional finite element analysis of the piston, are presented in Figure 10. Results for the two methods are the same, with a maximum difference of

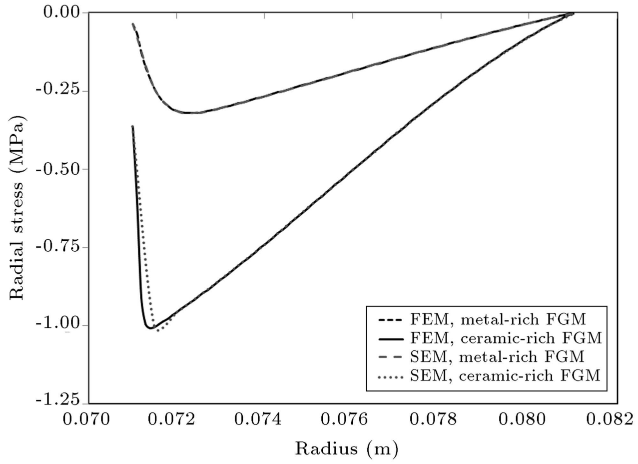

(a)

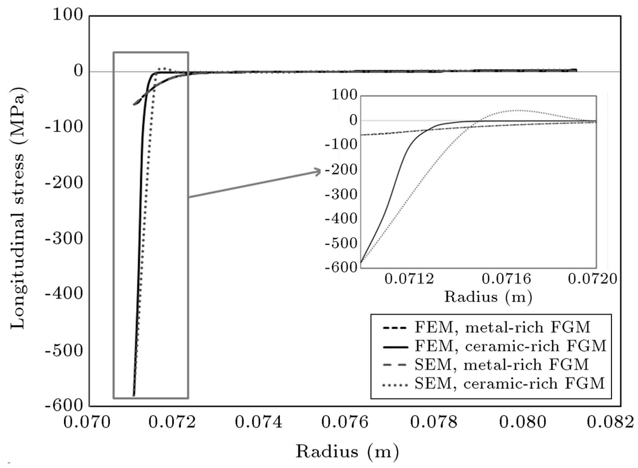

(b)

Figure 7. Distribution of (a) the radial stress and, (b) the longitudinal stress in the cylinder for the validation.

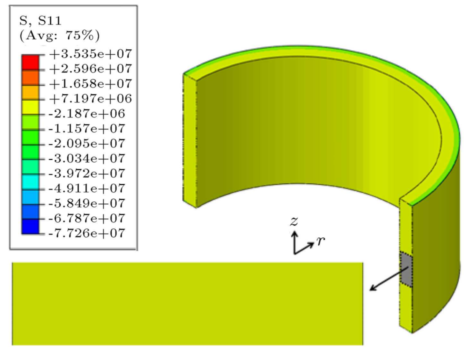

(a)

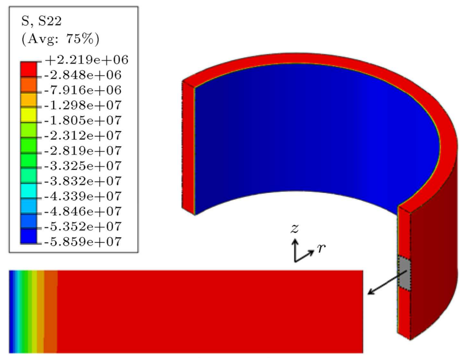

(b)

Figure 8. Distribution of (a) the radial stress and, (b) the longitudinal stress in the metal-rich cylinder obtained by the ABAQUS software.

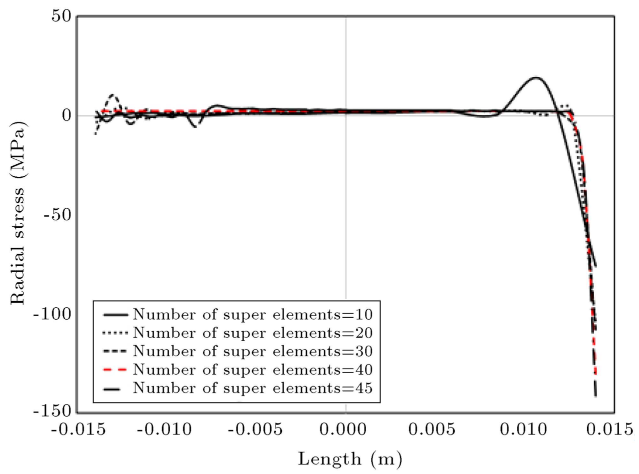

Figure 9. Distribution of the radial stress in the metal-rich piston for different numbers of super elements.

2%, while computational time with the super element is much less than with the conventional finite element. The radial and longitudinal stress distribution for a metal-rich piston is shown in Figure 11. As illustrated in these figures, the value of the longitudinal stress is lower than that of the radial stress, far from the boundary. The longitudinal stress is approximately uniform throughout the length of the piston. The radial stress is compressive on the top area of the piston, where the maximum temperature occurs, and then it becomes tensile in other regions.

3.5. SE results

Distribution of radial stress and longitudinal stress for different value powers of n in the FG cylinder are presented in Figure 12.

The radial stress is smaller in comparison with longitudinal stress, and the value of this stress is smaller than the combustion pressure. From the inner-out side of the cylinder, the radial stress increases in a compressive state and then decreases to zero on the outer radius of the cylinder, where there is no external pressure. As n_C increases, i.e. changing from pure metal to pure ceramic, the absolute value of the radial stress decreases for all values of cylinder radius. Changing the material of the cylinder from pure metal to pure ceramic leads to a decrease in radial stress, as well as an increase in longitudinal stress. However, as n_C increases, the longitudinal stress increases sharply, from 500 MPa to 1000 MPa, at the inner surface of the ceramic cylinder. By increasing n_C, a larger number of regions become ceramic, with higher elastic modulus. It is inferred that the effect of material distribution is more tangible on longitudinal stress than on radial stress.

Stress distribution versus length of piston for different values of n_P is demonstrated in Figure 13. The radial stress decreases by the enhancement of n_P. Higher amounts of n_P in the FG piston mean that the material will become softer (almost as a metal-rich material). For example, when n_P increases, radial stress increases sharply, from 600 MPa to 1100 MPa, on top of the piston. It is also observed that the

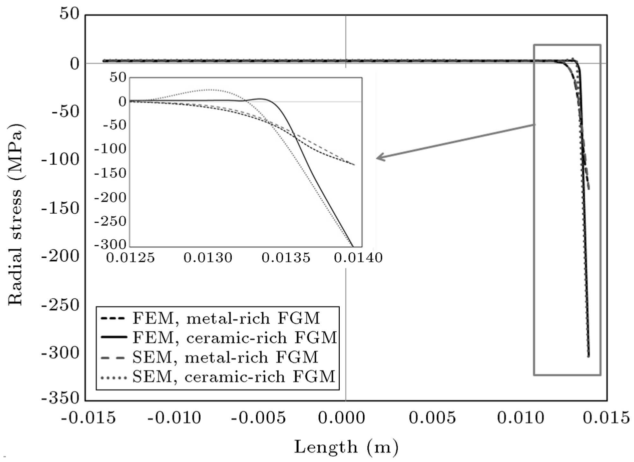

(a)

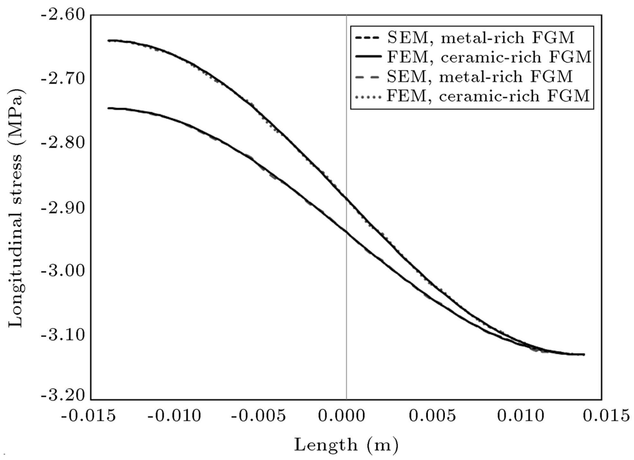

(b)

Figure 10. Distribution of (a) the radial stress and, (b) the longitudinal stress in piston for the validation.

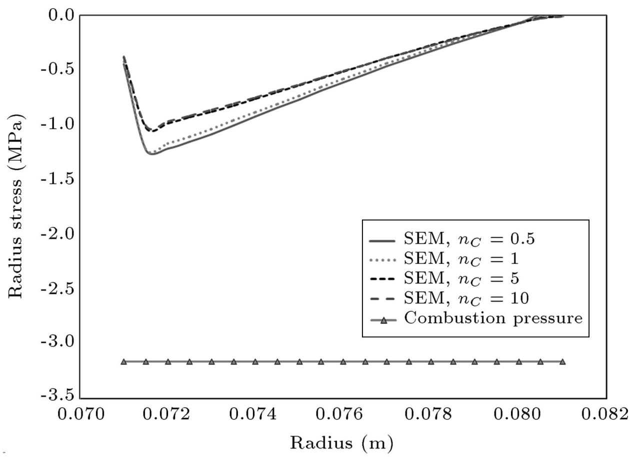

(a)

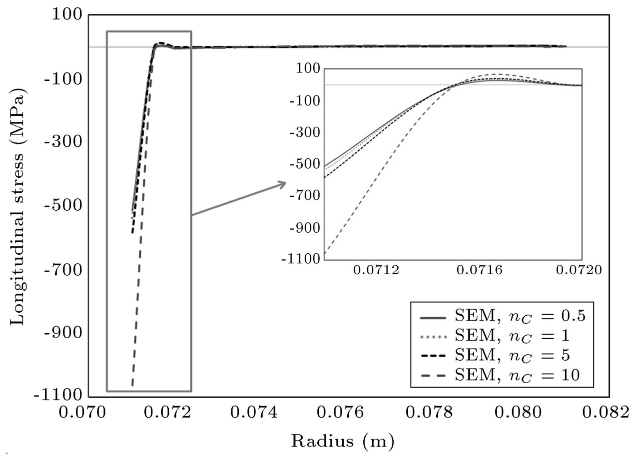

(b)

Figure 12. Distribution of (a) the radial stress and, (b) the longitudinal stress in the FG cylinder for different values of n by using the SEM.

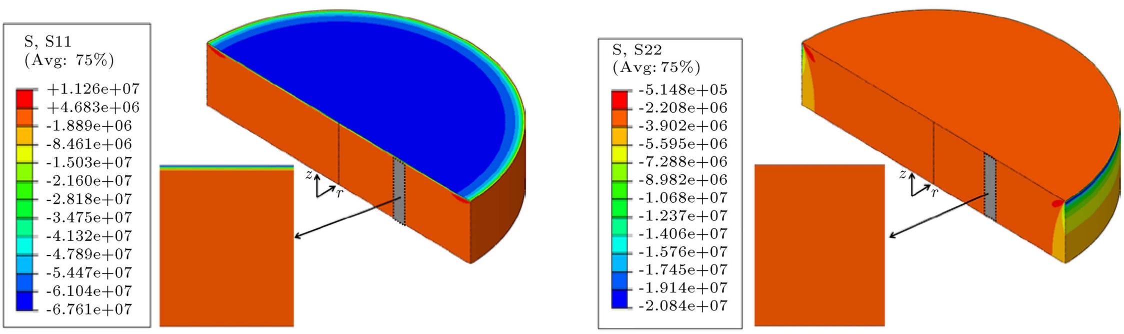

(a) (b)

Figure 11. Distribution of (a) the radial stress and, (b) the longitudinal stress in the metal-rich piston obtained by the ABAQUS software.

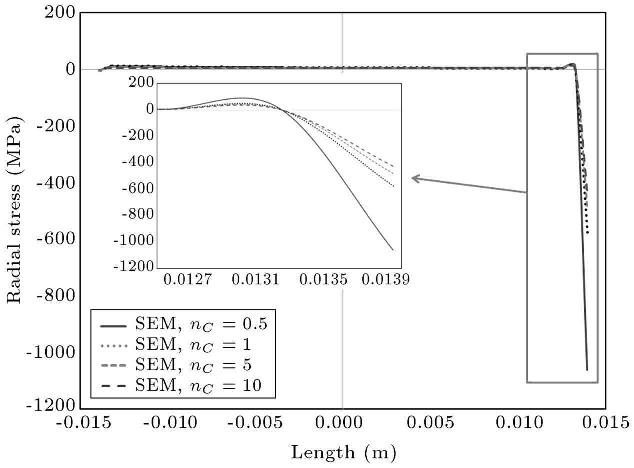

Figure 13. Radial stress distribution in the FG piston for different values of n_P by using the SEM.

effect of material distribution on radial stress is very significant.

4. Conclusion

In this paper, stress analysis of a FGM cylinder and piston of a combustion engine during the transient stage is performed. Effects of pressure and thermal stresses are included in the problem. A newly developed hollow cylindrical super element with 16 nodes is used for the analysis. The obtained results for simple cases, with uniform metal or ceramic materials, nicely matches the results obtained by the conventional finite element ABAQUS package. In the modeling with a super element, for similar findings, approximately five percent of the number of elements in the conventional finite element cylindrical type element is needed, while the time consumed is much less than in the conventional element.

Distribution of the material is assumed to be in the form of the power law. Considering the nonlinear temperature distribution in the cylinder, the thermal stresses at the internal surface of the cylinder are also nonlinear, which will be added to the pressure of the cylinder due to combustion. Findings also indicate that by changing the power of the material distribution, stress distribution can also be optimized.

References

1. Damircheli, M. and Azadi, M. "Temperature and thickness effects on thermal and mechanical stresses of rotating FG-disks", *Journal of Mechanical Science and Technology*, **25**(3), pp. 1-9 (2011).
2. Azadi, M. and Shariyat, M. "Nonlinear transient transfinite element thermal analysis of thick-walled FGM cylinders with temperature-dependent material properties", *Meccanica*, **45**(3), pp. 305-318 (2010).
3. Azadi, M. "Free and forced vibration analysis of FG-beam considering temperature dependency of material properties", *Journal of Mechanical Science and Technology*, **25**(1), pp. 69-80 (2011).
4. Sasaki, N., Nogawa, S. and Takahashi, D. "Engine cooling apparatus", Patent Application Number: 20120204820 (2012).
5. Moridi, A., Azadi, M. and Farrahi, G.H. "Thermo-mechanical stress analysis of thermal barrier coating system considering thickness and roughness effects", *Surface and Coatings Technology*, DOI: 10.1016/j.surfcoat.2012.02.019 (2012).
6. Arefi, M. "Nonlinear thermo-elastic analysis of thick-walled functionally graded piezoelectric cylinder", *Acta Mechanica*, **224**(11), pp. 2771-2783 (2013).
7. Dai, H.L. and Rao, Y.N. "Dynamic thermoelastic behavior of a double-layered hollow cylinder with an FGM layer", *Journal of Thermal Stresses*, **36**(9), pp. 962-984 (2013).
8. Feng, S.Z., Cui, X.Y., Li, G.Y., Feng, H. and Xu, F.X. "Thermo-mechanical analysis of functionally graded cylindrical vessels using edge-based smoothed finite element method", *International Journal of Pressure Vessels and Piping*, **111-112**, pp. 302-309 (2013).
9. Nie, G.J. and Batra, R.C. "Material tailoring and analysis of functionally graded isotropic and incompressible linear elastic hollow cylinders", *Composite Structures*, **92**(2), pp. 265-274 (2010).
10. Nie, G.J. and Batra, R.C. "Exact solutions and material tailoring for functionally graded hollow circular cylinders", *Journal of Elasticity*, **99**(2), pp. 179-201 (2010).
11. Safari, A., Tahani, M. and Hosseini, S.M. "Two-dimensional dynamic analysis of thermal stresses in a finite-length FG thick hollow cylinder subjected to thermal shock loading using an analytical method", *Acta Mechanica*, **220**(1-4), pp. 299-314 (2011).
12. Desai, P. and Kant, T. "A mixed semi analytical solution for functionally graded (FG) finite length cylinders of orthotropic materials subjected to thermal load", *International Journal of Mechanics and Materials in Design*, **8**(1), pp. 89-100 (2012).
13. Asemi, K., Akhlaghi, M. and Salehi, M. "Dynamic analysis of thick short length FGM cylinders", *Meccanica*, **47**(6), pp. 1441-1453 (2012).
14. Darabseh, T., Yilmaz, N. and Bataineh, M. "Transient thermo-elasticity analysis of functionally graded thick hollow cylinder based on Green-Lindsay model", *International Journal of Mechanics and Materials in Design*, **8**(3), pp. 247-255 (2012).
15. Akhlaghi, M., Zamani, A. and Hosseini, S.M. "Heat loss and thermal stresses in DI diesel engine using functionally graded cylinder (FGMs)", *Recent Advances in Composite Materials* (2007).

16. Koko, T.S. and Olson, M.D. "Vibration analysis of stiffened plates by super elements", *Journal of Sound and Vibration*, **158**, pp. 149-167 (1992).

17. Ahmadian, M.T. and Zahgeneh, M.S. "Application of super elements to free vibration analysis of laminated stiffened plates", *Journal of Sound and Vibration*, **259**(5), pp. 1243-1252 (2003).

18. Ahmadian, M.T. and Bonakdar, M. "A new cylindrical element formulation and its application to structural analysis of laminated hollow cylinders", *Finite Elements in Analysis and Design*, **44**, pp. 617-630 (2008).

19. Taghvaeipour, A., Bonakdar, M. and Ahmadian, M.T. "Application of a new cylindrical element formulation in finite element structural analysis of FGM hollow cylinders", *Finite elements in Analysis and Design*, **50**, pp. 1-7 (2012).

20. Azadi, M. and Azadi, M. "Nonlinear transient heat transfer and thermoelastic analysis of thick-walled FGM cylinder with temperature-dependent material properties using Hermitian transfinite element", *Journal of Mechanical Science and Technology*, **23**(10), pp. 2635-2644 (2009).

21. Mohammadi, A. *Heat Transfer Analysis on Engine Combustion Chamber by Using of KIVA Code*, Shiraz University, Shiraz, Iran (2007).

22. Pourhamid, R. and Mahdavy Moghaddam, H. "Thermal analysis of functionally graded materials in cylinders and pistons based on super element method", *Engine Research* (2014).

Appendix

Shape functions [19]:

$$N_1(\xi,\eta,\lambda) = \frac{1}{8}(\cos^2\pi\lambda - \cos\pi\lambda)(1+\xi)(1+\eta),$$

$$N_2(\xi,\eta,\lambda) = \frac{1}{8}(\cos^2\pi\lambda - \cos\pi\lambda)(1-\xi)(1+\eta),$$

$$N_3(\xi,\eta,\lambda) = \frac{1}{8}(\sin^2\pi\lambda - \sin\pi\lambda)(1+\xi)(1+\eta),$$

$$N_4(\xi,\eta,\lambda) = \frac{1}{8}(\sin^2\pi\lambda - \sin\pi\lambda)(1-\xi)(1+\eta),$$

$$N_5(\xi,\eta,\lambda) = \frac{1}{8}(\cos^2\pi\lambda + \cos\pi\lambda)(1+\xi)(1+\eta),$$

$$N_6(\xi,\eta,\lambda) = \frac{1}{8}(\cos^2\pi\lambda + \cos\pi\lambda)(1-\xi)(1+\eta),$$

$$N_7(\xi,\eta,\lambda) = \frac{1}{8}(\sin^2\pi\lambda + \sin\pi\lambda)(1+\xi)(1+\eta),$$

$$N_8(\xi,\eta,\lambda) = \frac{1}{8}(\sin^2\pi\lambda + \sin\pi\lambda)(1-\xi)(1+\eta),$$

$$N_9(\xi,\eta,\lambda) = \frac{1}{8}(\cos^2\pi\lambda - \cos\pi\lambda)(1+\xi)(1-\eta),$$

$$N_{10}(\xi,\eta,\lambda) = \frac{1}{8}(\cos^2\pi\lambda - \cos\pi\lambda)(1-\xi)(1-\eta),$$

$$N_{11}(\xi,\eta,\lambda) = \frac{1}{8}(\sin^2\pi\lambda - \sin\pi\lambda)(1+\xi)(1-\eta),$$

$$N_{12}(\xi,\eta,\lambda) = \frac{1}{8}(\sin^2\pi\lambda - \sin\pi\lambda)(1-\xi)(1-\eta),$$

$$N_{13}(\xi,\eta,\lambda) = \frac{1}{8}(\cos^2\pi\lambda + \cos\pi\lambda)(1+\xi)(1-\eta),$$

$$N_{14}(\xi,\eta,\lambda) = \frac{1}{8}(\cos^2\pi\lambda + \cos\pi\lambda)(1-\xi)(1-\eta),$$

$$N_{15}(\xi,\eta,\lambda) = \frac{1}{8}(\sin^2\pi\lambda + \sin\pi\lambda)(1+\xi)(1-\eta),$$

$$N_{16}(\xi,\eta,\lambda) = \frac{1}{8}(\sin^2\pi\lambda + \sin\pi\lambda)(1-\xi)(1-\eta).$$

Biographies

Reza Pourhamid received BS and MS degrees in Mechanical Engineering from Guilan University, Rasht, Iran, and Mazandaran University, Babol, Iran, in 2001 and 2005, respectively. He is currently a PhD degree candidate in the Science and Research Branch of the Islamic Azad University, Tehran, Iran. His research interests include heat transfer, combustion and thermoelasticity.

Mohammad Taghi Ahmadian received his BS and MS degrees in Physics, in 1972, from Shiraz University, in Iran. He also completed the requirements for BS and MS degrees in Mechanical Engineering receiving his MS degree in 1980 from the University of Kansas in Lawrence, USA. He also obtained PhD degrees in Physics and Mechanical Engineering, in 1980 and 1986, respectively, from the same institution. He is currently Professor in the School of Mechanical Engineering at Sharif University of Technology, Tehran, Iran, where he is also Head of the Bio-Engineering Center. His research interests include micro and nano mechanics, as well as bioengineering.

Hosein Mahdavy-Moghaddam received his PhD degree in Mechanical Engineering in 2000 from the University of Utah (Salt Lake City, Utah, USA), where he also taught under graduate courses. He is currently Assistant Professor in the Mechanical and Aerospace Engineering Department of the Science and Research

Branch of the Islamic Azad University, Tehran, Iran. His research interests are heat transfer and combustion.

Ali Reza Mohamadzadeh received his PhD degree in Mechanical Engineering from Michigan University, USA, and is currently Associate Professor and Head of the Mechanical Engineering Department in the Science and Research Branch of the Islamic Azad University, Tehran, Iran. His research interests include thermo-elasticity, thermo-magno-elasticity and nonlinear-dynamics and vibrations.